Available online at www.sciencedirect.com
ScienceDirect
Acta Materialia 58 (2010) 4012–4018
Acta MATERIALIA
www.elsevier.com/locate/actamat

First-principles calculations of the elastic, phonon and thermodynamic properties of $Al_{12}Mg_{17}$

H. Zhang *, S.L. Shang, Y. Wang, A. Saengdeejing, L.Q. Chen, Z.K. Liu

Department of Materials Science and Engineering, The Pennsylvania State University, University Park, PA 16802, USA

Received 8 September 2009; received in revised form 11 March 2010; accepted 12 March 2010
Available online 10 April 2010

Abstract

The elastic, phonon and thermodynamic properties of $Al_{12}Mg_{17}$ have been investigated by first-principles calculations. The obtained structural parameters, phonon dispersion curves and the predicted thermodynamic properties for all the phases studied herein agree well with available experimental data. The temperature-dependent single-crystal elastic constants are also predicted along with the polycrystalline aggregate properties, including bulk modulus, shear modulus, Young's modulus, and Poisson's ratio. The brittleness of $Al_{12}Mg_{17}$ that we predict is consistent with experiments, in contrast to the previous calculation showing ductile behavior. Detailed analysis of density of states further explains the present theoretical findings.

Keywords: First-principles electron theory; Intermetallic compounds; Elastic behavior; Thermodynamics

1. Introduction

As lightweight structural materials with a good combination of castability and mechanical properties, Al–Mg-based alloys have been applied extensively in the automotive and aerospace industries [1–3]. For example, the (Mg–(2–6)% Al) alloy and the AZ91 alloy (Mg–9% Al–1% Zn) show good performance at room temperature [1]. In those alloys, the γ-$Al_{12}Mg_{17}$ phase is the essential intermetallic phase and plays an important role in the strengthening of the alloys at room temperature. However, the existence or creep-induced precipitation of the γ-$Al_{12}Mg_{17}$ phase greatly damages the creep property of Al–Mg-based alloys at elevated temperatures and hence limits their applications [4]. Although many experimental studies on crystal structure and precipitation of $Al_{12}Mg_{17}$ in the Al–Mg system have been undertaken in the past decades [5–7], knowledge of the thermodynamic and mechanical properties of this phase is still incomplete.

The present work aims to investigate in detail the structure, mechanical, phonon, and thermodynamic properties of $Al_{12}Mg_{17}$ from first-principles calculations within density functional theory [8]. First, we investigate the structural properties of $Al_{12}Mg_{17}$. By using the supercell method [9], the first-principles phonon calculations of those phases are carried out. The phonon density of states (DOSs) are subsequently used to calculate the vibrational contributions to the total free energy and the finite temperature thermodynamic properties. As indicated by Wang et al. [10], the thermal electronic contributions are important for metals, and we thus include it in the present work. The thermodynamic properties of $Al_{12}Mg_{17}$, such as heat capacity, and thermal expansion are then predicted and compared with available experimental data in the literature. Furthermore, the temperature dependency of single-crystal elastic constants and correspondingly bulk modulus, shear modulus, Young's modulus, and Poisson's ratio are predicted and compared with the available experiments. It is expected that this study will provide useful guidance for both analysis and design of the Al–Mg-based alloys containing $Al_{12}Mg_{17}$.

* Corresponding author. Tel.: +1 814 865 9957.
E-mail address: huz106@psu.edu (H. Zhang).

1359-6454/$36.00
doi:10.1016/j.actamat.2010.03.020

The rest of the paper is organized as follows. In Section 2, the theories of the calculations of elastic, phonon, and thermodynamic properties are introduced. The computational framework and simulation details are described in Section 3. In Section 4, we discuss the obtained thermal, physical, and mechanical properties of $Al_{12}Mg_{17}$ and finally report our conclusions.

2. Theory

The Helmholtz free energy of a system, F, at temperature T and volume V is given by [10–12]:

$$F(V,T) = E_0(V) + F_{vib}(V,T) + F_{el}(V,T) \quad (1)$$

where E_0 (V) is the first-principles static energy at 0 K and volume V, $F_{vib}(V, T)$ the lattice vibrational contributions to the free energy, and $F_{el}(V, T)$ the thermal electronic contributions. Within the quasiharmonic approximation, the anharmonic effect is accounted by the harmonic approximation at several volumes. From the phonon density of states, the lattice vibrational free energy can be calculated [10–12].

In the present work, the elastic stiffness c_{ij}'s are calculated based on the stress–strain method [13]. This methodology involves a set of strains $\boldsymbol{\varepsilon} = (\varepsilon_1\ \varepsilon_2\ \varepsilon_3\ \varepsilon_4\ \varepsilon_5\ \varepsilon_6)$ where ε_1, ε_2, and ε_3 refer to the normal strains, and ε_4, ε_5, ε_6 the shear strains. Set of strains are imposed on a crystal with lattice vectors $\mathbf{R}$ specified in Cartesian coordinates. After the strains are applied, the deformed lattice vectors $\overline{\mathbf{R}}$ are obtained. Using the matrix notation for elasticity and the general Hooke law, the stresses ($\boldsymbol{\sigma}$) cased by the application of strains (ε) are related by the following:

$$\boldsymbol{\sigma} = \boldsymbol{\varepsilon}\mathbf{C} \quad (2)$$

where $\mathbf{C}$ is the 6×6 elastic stiffness matrix with elements c'_{ij}s in Voigt's notation. $\boldsymbol{\sigma}$ can be obtained by first-principles calculations. From n sets of strains and the resulting stresses, the elastic constants $\mathbf{C}$ can be calculated by:

$$\mathbf{C} = \boldsymbol{\varepsilon}^{-1}\boldsymbol{\sigma} \quad (3)$$

where -1 represents the pseudo-inverse, which can be solved by the singular value decomposition method. Two independent sets of strains are employed here since $Al_{12}Mg_{17}$ has a cubic structure. The independent set of strains is applied in the following form:

$$\begin{pmatrix} x & 0 & 0 & 0 & 0 & 0 \\ 0 & x & 0 & 0 & 0 & 0 \\ 0 & 0 & x & 0 & 0 & 0 \\ 0 & 0 & 0 & x & 0 & 0 \\ 0 & 0 & 0 & 0 & x & 0 \\ 0 & 0 & 0 & 0 & 0 & x \end{pmatrix} \quad (4)$$

For the purposes of accuracy, elastic constants with the 0 K equilibrium volume were performed under additional sets of strains with $x = \pm 0.007$, ± 0.01 and ± 0.013 to evaluate the numerical error. For calculations at other volumes, two strains with $x = \pm 0.01$ are chosen. More details about the stress vs. strain method and its applications to determine c_{ij}'s can be found in, for example, Refs. [13] (Al_2O_3), [14,15] (Mg-based alloys), [16] (Ni), [17] ($BiFeO_3$) and [18] (Fe_3C).

The temperature dependence of elastic stiffness is obtained by combination of the volume dependence of elastic stiffness and the temperature dependence of volume from the minimization of Helmholtz free energy (Eq. (1)) at given temperatures. First, we calculate $c_{ij}(V)$ at different volumes. Second, the equilibrium volume at various temperatures is determined from Helmholtz free energy as described in Eq. (1), with both lattice vibrational and thermal electronic contributions included. The combination of $c_{ij}(V)$ and $V(T)$ leads to the temperature dependence of elastic constants $c_{ij}(T)$.

In the above procedure, the elastic stiffness coefficients are obtained under isothermal conditions (c_{ij}^T). However, most of the experimental elastic stiffness coefficients are measured by resonant vibrations under isentropic conditions (c_{ij}^S). To make them comparable, c_{ij}^T could be converted to c_{ij}^S according to the relations discussed by Davies [19] as follows:

$$c_{ij}^S = c_{ij}^T + \frac{T\lambda_i\lambda_j}{\rho C_\varepsilon} \quad (5)$$

$$\lambda_i = -\sum_j \alpha_j c_{ij}^T \quad (6)$$

where ρ is the density, C_ε the heat capacity under constant strain, and α_j the thermal expansion.

The conversion from c_{ij}^T to c_{ij}^S has been applied to both pure metallic elements and binary alloys like Mg–3 wt.% Al, Mg–9 wt.% Al [20], face-centered cubic (fcc) Cu, Al, NiAl [21] and body-centered cubic (bcc) Ta [22].

3. Computational details

The electronic structure and total energies of $Al_{12}Mg_{17}$ are calculated by using the projector-augmented wave (PAW) method as implemented in VASP [23,24]. The generalized gradient approximation (GGA) of Perdew–Burke–Ernzerhof (PBE) [25] is used for the exchange–correlation functional. The electronic configurations considered are $3s^23p^1$ for Al, and $2p^63s^2$ for Mg, respectively. $Al_{12}Mg_{17}$ is the cubic structure with Pearson's symbol of $cI58$ and space group $I\bar{4}3m$ [26]. We use the energy cutoff of 350 eV, i.e., 1.3 times the highest energy cutoff between Al, and Mg suggested by VASP. The Monkhorst–Pack scheme is used for the Brillouin-zone integrations [27], and k-mesh of $6 \times 6 \times 6$ is used to calculate the electronic structure. The phonon calculations are carried out by the supercell method [9,28], as implemented in the ATAT code [9], with 58 atoms in the supercell. The phonon calculations are performed with k-mesh of $4 \times 4 \times 4$, 0.1 is employed for the setting of displacement from the equilibrium atomic position, and the cutoff distance of 5 is used to fit the force constants. We carried out systematic tests in terms of the

above first-principles calculations parameters and found out that the calculated elastic stiffness constants are well converged.

4. Results and discussion

4.1. Structure and vibrational properties

The total energy as a function of volume is calculated and fitted by the four parameters modified Birch–Murnaghan equation of state [29–32]:

$$E(V) = a + bV^{-1/3} + cV^{-2/3} + dV^{-1} \quad (7)$$

where a, b, c, and d are fitting parameters. Herein the equilibrium volume, bulk modulus and its pressure derivative for $Al_{12}Mg_{17}$ at 0 K are derived and listed in Table 1. All predicted properties are in good agreement with experimental measurements. To validate the first-principles phonon calculations, one of the most important steps is to calculate the phonon dispersions. Fig. 1 shows the phonon dispersion relations for $Al_{12}Mg_{17}$ at its experimental equilibrium volume at 298 K.

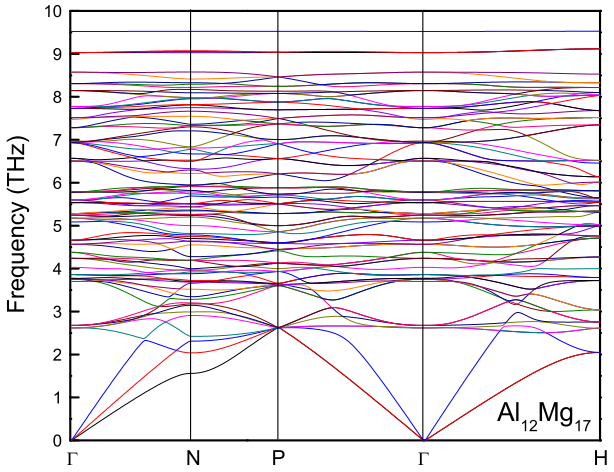

Fig. 1. Calculated phonon dispersion curves for $Al_{12}Mg_{17}$ pertaining to the equilibrium lattice parameters at 298 K.

4.2. Thermodynamic properties

Starting from both the electronic and phonon DOSs at several different volumes, the free energies (F) can be predicted based on the quasiharmonic approximation, i.e., Eq. (1). In this work, the first-principles calculations are carried out at $P = 0$ and hence $PV = 0$; as a result, the Helmholtz free energy is equal to the Gibbs energy. The lattice vibrational entropy and thermal electronic entropy can be calculated accordingly, and the summation of these two parts gives the total entropy.

Fig. 2 shows the predicted S and G, where the reference state for H is the commonly used setting in the thermochemistry community, i.e., at 298.15 K and 1 bar for the stable structure of pure elements. It is shown that there is only slight difference between the calculated values with and without the thermal electronic contribution, and the value of S taken into thermal electronic contribution is slightly higher. Using the results shown in Fig. 2, the enthalpy of formation for $Al_{12}Mg_{17}$ at 298 K can be predicted as shown in Table 1. Experimentally determined values by Brown and Pratt [33] and by Predel and Hulse [34] do not agree with each other. Our calculated value falls between these two sets of data and has a reasonable agreement with the value obtained by Zhong et al. [35] with the difference about 0.9 kJ (mol. atom)$^{-1}$. Table 1 also presents the calculated structure parameters at 298 K compared with available experiments [26,33–35].

Table 1
Calculated properties of $Al_{12}Mg_{17}$ at 0 K and 298 K (with both phonon and thermal electronic contributions). The results include lattice parameters (a_0), equilibrium volume (V), bulk modulus (B_0), pressure derivative of bulk modulus (B_0'), enthalpy of formation ΔH, heat capacity (C_P), and linear thermal expansion (α_L).

	0 K			298 K	
	Calc.	Exp.		Calc.	Exp.
a_0 (Å)	10.53	10.54[a]	V_{298} (Å^3 atom^{-1})	20.61	20.19
V_0 (Å^3 atom^{-1})	20.15	20.19	ΔH (kJ (mol. atom))$^{-1}$	−2.64	−3.78[c], −0.97[d], −3.58[e]
B_0 (GPa)	49.53	49.6[b]	B^T (GPa)	44.3	
B_0'	4.44		B^S (GPa)	45.7	
			C_P (J mol^{-1} K^{-1})	24.4	
			α_L (10^{-6} K^{-1})	23.9	

[a] The experimental lattice parameters are reported at room temperature [26].
[b] Calculated value [37].
[c] Experimental data by Brown and Pratt [33].
[d] Experimental data by Predel and Hulse [34].
[e] Calculated value from Ref. [35].

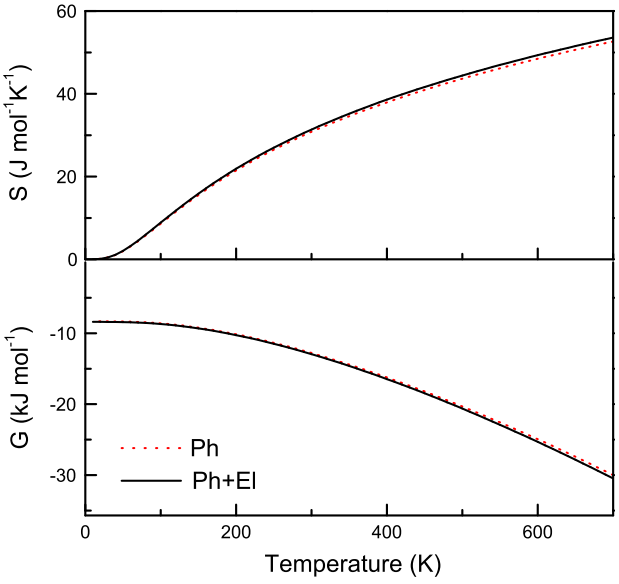

Fig. 2. Thermodynamic properties: entropy (S) and Gibbs energy (G) for $Al_{12}Mg_{17}$. The solid lines and dotted lines are the calculated results with (Ph + El) and without (Ph) the thermal electronic contributions, respectively.

Once the phonon spectrum over the entire Brillouin zone is available, the vibrational heat capacity (C_V^{vib}) and the thermal electronic contribution to heat capacity (C_V^{el}), both at constant volumes, can be obtained. Consequently, the heat capacity at constant pressure, C_P, can be computed as

$$C_P = C_V^{vib} + C_V^{el} + \alpha_V^2 BVT \tag{8}$$

where α_V is the volume thermal expansion coefficient, and B the bulk modulus. Table 1 shows the predicted heat capacities of $Al_{12}Mg_{17}$ at 298 K. C_P of $Al_{12}Mg_{17}$ with and without the thermal electronic contributions are plotted in Fig. 3. Considering the contributions to the heat capacity from the terms in Eq. (8), C_V^{vib} tends to the classical constant $3R$ while C_V^{el} keeps increasing with increasing temperature. It could be seen that the contribution from C_V^{el} increases with increasing temperature. At 700 K, there is 1.81% difference of C_P with and without C_V^{el} for $Al_{12}Mg_{17}$.

The linear thermal expansion coefficient α_L at a fixed pressure ($P = 0$ in the present work) is given by:

$$\alpha_L = \frac{1}{3}\alpha_V = \frac{1}{3V}\left(\frac{\partial V}{\partial T}\right)_P \tag{9}$$

The calculated linear thermal expansion coefficients with both vibrational and thermal electronic contributions are shown in Table 1 at 298 K, and plotted in Fig. 4. The thermal electronic contribution to the thermal expansion coefficient is relatively small: the difference is about 0.89% for $Al_{12}Mg_{17}$ at 700 K. The obtained thermal expansion of $Al_{12}Mg_{17}$ is likely to be overestimated, which was also noticed in other systems like Al and Ni [10], and this larger disparity at higher temperatures is possibly due to the limitations of the current quasiharmonic approximation. Grabowski et al. [36] recently concluded that the anharmonic contribution to the free energy has a significant influence on thermal expansion coefficient at high temperatures, and quantitatively predicted anharmonic contribution to

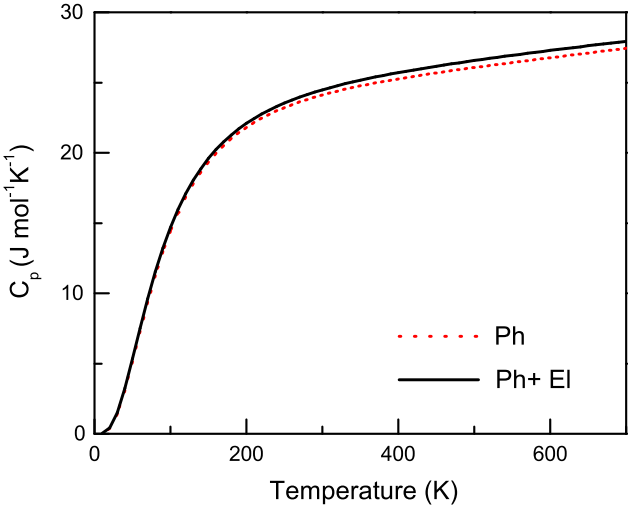

Fig. 3. Temperature dependence of heat capacity of $Al_{12}Mg_{17}$. Solid and dashed curves show the calculated C_P, with and without thermal electronic contribution, respectively.

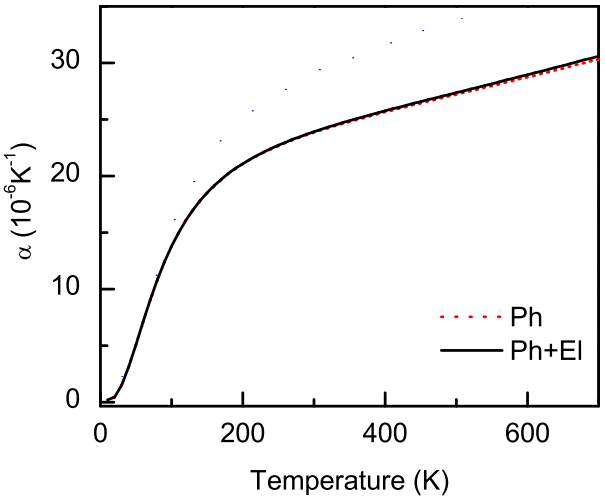

Fig. 4. Temperature dependence of lineal thermal expansion for $Al_{12}Mg_{17}$. Solid and dashed curves show the calculated thermal expansion, with and without thermal electronic contribution, respectively.

α is shifted downward by −6% at 700 K for Al. Another reason for this disparity at high temperatures is that the GGA calculation underestimates bulk modulus and hence overestimates thermal expansion.

The isothermal bulk modulus can be calculated as a function of temperature as:

$$B^T(V,T) = \frac{1}{V}\left(\frac{\partial^2 F(V,T)}{\partial V^2}\right)_T \tag{10}$$

Denoting C_P/C_V by γ, we have $\gamma B^T = B^S$, and the ratio of C_P to C_V is the ratio of the isentropic bulk modulus (B^S) to the isothermal bulk modulus (B^T). From this, we can conclude that B^S is always greater than B^T, and they are equal at 0 K. The temperature dependences of both B^T and B^S for $Al_{12}Mg_{17}$ are shown in Fig. 5, and the calculated results at 298 K are listed in Table 1. The calculated bulk modulus with and without thermal electronic contribution is almost identical (less than 0.2% at 700 K) so the latter case is excluded in Fig. 5, different from previous figures (Figs. 3 and 4) where both cases are presented.

4.3. Elastic properties

The calculated c_{ij}^T's and c_{ij}^S's of $Al_{12}Mg_{17}$ at both 0 K and 298 K are listed in Table 2. Note that c_{ij}^T and c_{ij}^S are equal at 0 K from Eq. (5). Table 2 also lists the absolute uncertainty for each property of $Al_{12}Mg_{17}$ at 0 K, which is treated as the maximum value of $|A_i - A_{avg}|$, where A_i is the calculated value and A_{avg} the average value. We also compute the relative deviation through $\sqrt{\frac{\sum_i [(c_i - c_{avg})/c_{avg}]^2}{3}}$ where c_i is the calculated elastic constant from each $|x|$, and c_{avg} the average value. The relative deviations are 0.4%, 1.3%, and 4.7%, for c_{11}, c_{12} and c_{44} at 0 K, respectively, indicating the good predictions of c_{ij}. We note that $c_{ij}^T \leqslant c_{ij}^S$ except isothermal c_{44}^T and isentropic c_{44}^S are equal. In Table 2, the previous calculation for $Al_{12}Mg_{17}$ [37] are

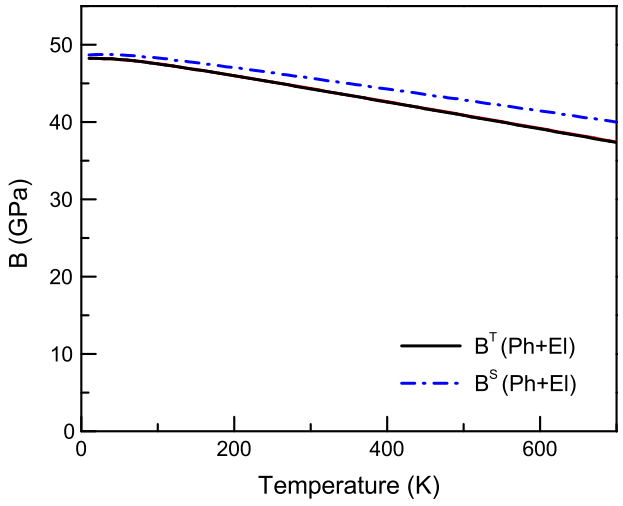

Fig. 5. Temperature dependence of bulk modulus for $Al_{12}Mg_{17}$. Solid and dashed curves show the B^T and B^S, respectively.

included for comparison. The elastic moduli of these phases, bulk modulus (B) and shear modulus (G), can be calculated using single-crystal constants by the following equations:

$$B = (c_{11} + 2c_{12})/3 \quad (11)$$

$$G = (c_{11} + c_{12} + 3c_{44})/5. \quad (12)$$

It is worth mentioning that the value of bulk modulus derived from elastic constants by Eq. (11) has a good agreement with the ones obtained by Eq. (10) (Table 1). Furthermore, Table 2 also summarizes the properties derived from calculated elastic constants of $Al_{12}Mg_{17}$ at 298 K, including Young's modulus, Poisson's ratio, and B/G ratio. Young's modulus (E), the evaluation of the stiffness of the solid, is defined as $E = (9BG)/(G + 3B)$. $Al_{12}Mg_{17}$ has a larger value of Young's modulus than both Al and Mg, indicating that $Al_{12}Mg_{17}$ is stiffer than both pure Al and Mg. Poisson's ratio v is employed to indicate the stability of the crystal against shear stress. The calculated results show that compared with the Al and Mg, $Al_{12}Mg_{17}$ has a lower tenacity since it has a smaller value of Poisson's ratio v. It is also known that B/G introduced by Pugh [38] is associated with ductility (brittleness), where B is considered as the resistance to fracture, and G the resistance to plastic deformation. The critical value which separates ductile and brittle is about 1.75. The calculated results show that $Al_{12}Mg_{17}$ is brittle, which is in contrast to the previous prediction made by Wang et al. [37]. As expected, the derived mechanical properties from elastic constants are also notably different from the previous calculation. For example, Wang et al. [37] calculated $B/G = 2.19$ and hence predicted $Al_{12}Mg_{17}$ to be ductile. However, our prediction of the brittleness of $Al_{12}Mg_{17}$ is confirmed by several experimental observations [39–41].

To obtain a better understanding of the mechanical properties of $Al_{12}Mg_{17}$, the electronic structure is calculated and shown in Fig. 6 as well as the total density of states of $Al_{12}Mg_{17}$ and its angular-moment decomposition plots for Mg and Al. The total densities of states for Al and Mg in $Al_{12}Mg_{17}$ are compared with the ones in pure Al and Mg. The comparison reveals that the DOSs below the Fermi level for the Al atoms in $Al_{12}Mg_{17}$ become more localized than those in pure Al. This observation suggests that hybridization between Al and Mg increases the bonding directionality of Al, implying that the covalent-like bonding existed in $Al_{12}Mg_{17}$. As the localization of bonding electrons is the dominant factor in governing the brittleness of the materials, the brittle behavior of $Al_{12}Mg_{17}$ can be explained.

Fig. 7 shows temperature dependences of both c_{ij}^T and c_{ij}^S of $Al_{12}Mg_{17}$. Values of elastic constants decrease monotonically with the increase of temperature. Two sets of bulk modulus, shear modulus, and Young's modulus as a function of temperature derived by c_{ij}^T and c_{ij}^S, respectively, are shown in Fig. 8. It is noted that the temperature dependence of bulk modulus derived by elastic constants is similar to the ones from Eq. (10) as in Fig. 5, showing a consistent estimation of the compressibility of this phase.

5. Conclusions

In this work, a comprehensive analysis of the structural, electronic, and vibrational properties of $Al_{12}Mg_{17}$ has been performed from first-principles. The calculated equilibrium lattice constant is in good agreement with experimental data. The thermodynamic properties of $Al_{12}Mg_{17}$ are calculated within the quasiharmonic approximation, and the thermal electronic contribution due to thermal excitation is considered. The finite temperature thermodynamic properties of thermal expansion, heat capacities, and bulk modulus are calculated. We have studied the temperature dependence of the single-crystal elastic constants as well as polycrystalline elastic properties (B, G, E and v) from first-principles. They indicate

Table 2
Calculated c_{ij}^T's and c_{ij}^S's (GPa) of $Al_{12}Mg_{17}$ at both 0 K and 298 K compared with previous calculation.

	c_{11}	c_{12}	c_{44}	B	G	E	v	B/G
$c_{ij}^T(298)$	92.0	26.1	30.7	48.1	31.6	77.8	0.23	1.52
$c_{ij}^S(298)$	93.3	27.4	30.7	49.4	31.6	78.1	0.24	1.56
$c_{ij}^T(0)$	97.7 ± 0.8	28.1 ± 0.5	31.4 ± 1.1	51.3 ± 0.4	32.7 ± 1.0	81.0 ± 2.2	0.24 ± 0.01	1.57 ± 0.04
Ref.[a]	86.8	29	20	48.3	22	57.3	0.3	2.19

[a] Ref. [37], the calculated value at 0 K.

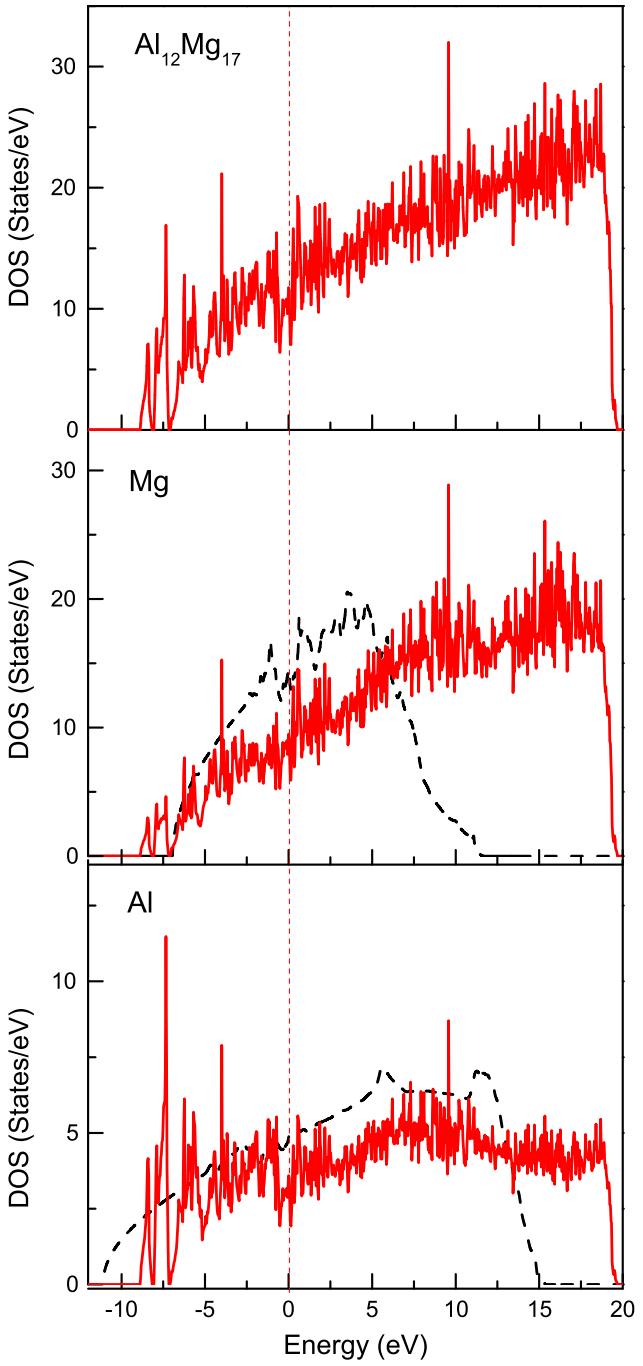

Fig. 6. Calculated total densities of states (DOSs) for $Al_{12}Mg_{17}$ and angular-momentum decomposition of Al and Mg. The solid lines are for Al or Mg in $Al_{12}Mg_{17}$ bulk and dashed lines are for pure Al or Mg bulk. The dotted line dictates Fermi level.

that $Al_{12}Mg_{17}$ is stiffer than Al and Mg and has a lower tenacity with a smaller Poisson's ratio. In contradiction to the previous elastic constant calculation [37], we predicted that $Al_{12}Mg_{17}$ is brittle. We have demonstrated that the brittle behavior of $Al_{12}Mg_{17}$ is due to the localization of bonding electrons of Al. Our result of brittleness of $Al_{12}Mg_{17}$ is supported by the experimental observations [39–41].

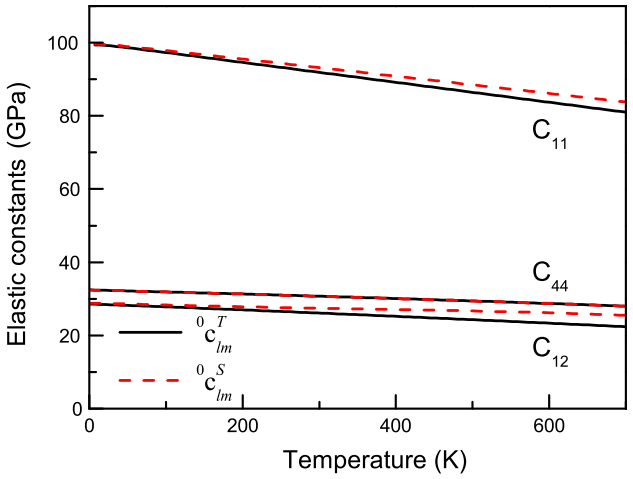

Fig. 7. Temperature dependence of elastic constants for $Al_{12}Mg_{17}$. Solid and dashed curves show the calculated c_{ij}^T and c_{ij}^S, respectively.

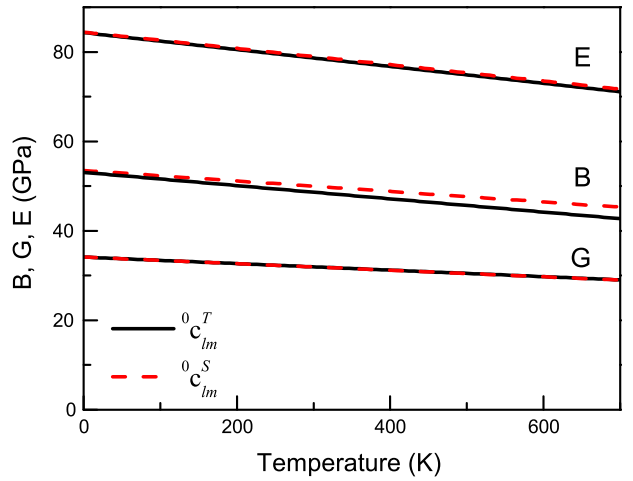

Fig. 8. Calculated bulk modulus, shear modulus, and Young's modulus as a function of temperature. Solid and dashed curves show the results derived from c_{ij}^T and c_{ij}^S, respectively.

Acknowledgements

This work was funded by the National Science Foundation (NSF) through Grant No. DMR-0510180. First-principles calculations were carried out partially on the LION clusters supported by the Materials Simulation Center and the Research Computing and Cyber infrastructure unit at Pennsylvania State University, and partially on the resources of NERSC supported by the Office of Science of the US DOE under Contract No. DE-AC02-05CH11231.

References

[1] Luo A. Materials comparison and potential applications of magnesium in automobiles. In: Clow BB, editor. Magnesium technology 2000. Nashville (TN): Minerals, Metals and Materials Society/AIME, PA; 2000. p. 89–100.
[2] Shang S, Zhang H, Ganeshan S, Liu ZK. JOM 2008;60:45.

[3] Du Y, Wang J, Zhao JR, Schuster JC, Weitzer F, Schmid-Fetzer R, et al. Int J Mater Res 2007;98:855.
[4] Luo A, Pekguleryuz MO. J Mater Sci 1994;29:5259.
[5] Celotto S. Acta Mater 2000;48:1775.
[6] Duly D, Zhang WZ, Audier M. Philos Mag A 1995;71:187.
[7] Zhang MX, Kelly PM. Acta Mater 2005;53:1085.
[8] Kohn W, Sham L. Phys Rev 1965;140:1133.
[9] van de Walle A, Asta M, Ceder G. CALPHAD 2002;26:539.
[10] Wang Y, Liu ZK, Chen LQ. Acta Mater 2004;52:2665.
[11] Baroni S, de Gironcoli S, Dal Corso A, Giannozzi P. Rev Mod Phys 2001;73:515.
[12] Shang S, Wang Y, Arroyave R, Liu ZK. Phys Rev B 2007;75:092101.
[13] Shang SL, Wang Y, Liu ZK. Appl Phys Lett 2007;90:101909.
[14] Ganeshan S, Shang SL, Wang Y, Liu ZK. Acta Mater 2009;57:3876.
[15] Ganeshan S, Shang SL, Zhang H, Wang Y, Mantina M, Liu ZK. Intermetallics 2009;17:313.
[16] Kim D, Shang SL, Liu ZK. Comput Mater Sci 2009;47:254.
[17] Shang SL, Sheng G, Wang Y, Chen LQ, Liu ZK. Phys Rev B 2009;80:052102.
[18] Nikolussi M, Shang SL, Gressmann T, Leineweber A, Mittemeijer E, Wang Y, et al. Scripta Mater 2008;59:814.
[19] Davies GF. J Phys Chem Solids 1974;35:1513.
[20] Liu ZK, Zhang H, Ganeshan S, Wang Y. Scripta Mater; in press. doi:10.1016/j.scriptamat.2010.03.049.
[21] Wang Y, Wang JJ, Zhang H, Manga VR, Shang SL, Chen LQ, Liu ZK. 2010, unpublished.
[22] Gulseren O, Cohen RE. Phys Rev B 2002;65:064103.
[23] Kresse G, Furthmuller J. Comput Mater Sci 1996;6:15.
[24] Kresse G, Furthmuller J. Phys Rev B 1996;54:11169.
[25] Perdew JP, Wang Y. Phys Rev B 1992;45:13244.
[26] Villars PP. Pearson's handbook of crystallographic data for intermetallic phases. American Society for Metals; 1985.
[27] Monkhorst HJ, Pack JD. Phys Rev B 1976;13:5188.
[28] Arroyave R, Shin D, Liu ZK. Acta Mater 2005;53:1809.
[29] Birch F. J Geophys Res 1978;83:1257.
[30] Shang S, Bottger A. Acta Mater 2005;53:255.
[31] Teter DM, Gibbs GV, Boisen MB, Allan DC, Teter MP. Phys Rev B 1995;52:8064.
[32] Shang SL, Wang Y, Kim DE, Liu ZK. Comput Mater Sci 2010;47:1040.
[33] Brown JA, Pratt JN. Metall Trans 1970;1:2743.
[34] Predel B, Hulse K. Z Metallkd 1978;69:661.
[35] Zhong Y, Yang M, Liu ZK. CALPHAD 2005;29:303.
[36] Grabowski B, Ismer L, Hickel T, Neugebauer J. Phys Rev B 2009;79:134106.
[37] Wang N, Yu WY, Tang BY, Peng LM, Ding WJ. J Phys D: Appl Phys 2008;41:195408.
[38] Pugh SF. Philos Mag 1954;45:823.
[39] Cai J, Ma GC, Liu Z, Zhang HF, Hu ZQ. J Alloy Compd 2006;422:92.
[40] Gu XY, Sun DQ, Liu L. Mater Sci Eng A 2008;487:86.
[41] Prakash DGL, Regener D, Vorster WJJ. Mater Sci Eng A 2008;488:303.